Geophys. J. R. astr. Soc. (1970) **21**, 65–78.

Stress and Deflection in the Lithosphere near Lake Kariba—I

D. I. Gough and W. I. Gough

(Received 1970 March 26)

Summary

Calculations of incremental stress and deflection in the crust have been made as part of a study of load-induced seismic activity at Lake Kariba. A general method is described for computing any desired stress components anywhere in an elastic half-space near a load of any shape on its surface. The program also computes the elastic depression and the gravitational energy converted to stored elastic strain energy. The static incremental stress and depression in the lithosphere near Lake Kariba are discussed with the aid of vertical sections and maps. The maximum shear stress under the deepest part of the lake rises to 2·12 bars, and the downward normal stress to 6·68 bars. The maximum depression in the Sanyati Basin is 23·5 cm. Computed depression differences along the Makuti–Kariba road are shown to be in excellent agreement with results of repeated precise levelling. The deflection is therefore mainly elastic and Young's modulus is near 0·85 megabars for the lithosphere in the area. Some evidence is available which suggests vertical movements of blocks on fault planes, no doubt associated with the earthquakes. Extended relevelling should give results of great scientific and engineering value. Stress differences produced by the lake in the upper mantle are too small to produce flow there, so that inelastic depression of the crust toward isostatic compensation of the load is not to be expected.

1. Introduction

Considerable seismic activity followed the filling, in 1963, of the world's largest artificial lake on the Zambezi River upstream from a dam at Kariba, Rhodesia. This induced seismicity is discussed in an accompanying paper (Gough & Gough 1970) hereafter referred to as Paper II. Evidence is there offered that the seismicity is a result of re-activation of existing faults in the rift valley which contains the lake. It is further argued that the activity has occurred through addition of small stresses caused by the load to larger initial stresses, and not through the effects of fluid pressure. As part of the investigation a study has been made of the incremental stress, elastic vertical depression and release of gravitational potential energy brought about by the filling of Lake Kariba. This study is reported in the present paper.

One of us has given a method of calculating incremental stress under a two-dimensional artificial lake (Gough 1969). This method could have been applied to sections through the crust under central parts of Lake Kariba. To allow evaluation

of stresses near the deep end of the lake, and in particular estimation of the volume of rock stressed above a chosen value, a general three-dimensional method has been evolved.

2. Bathymetry of Lake Kariba

A detailed bathymetric chart of the lake on a scale of 1 : 100,000, published by the Surveyor General of Rhodesia, has been used for estimation of mean water depths in squares as described in Section 3. Fig. 1 gives the general form of the lake by means of the shoreline and contours, smoothed from the 1 : 100,000 chart, at depths 40 and 70 metres. Depth is taken from the normal maximum water level, 484·6 m (1590 feet) above sea level. The lake level has risen to a peak value of 487·5 m (at the time of maximum seismicity) and drops to between 480 and 483 m annually during the dry season. The area of maximum load, near the north shore and westward from Kariba Dam, is known as the Sanyati Basin. A narrow waist in the lake divides an upper basin from a lower basin of which the Sanyati Basin forms the maximum development.

The numbered lines in Fig. 1 give the positions of vertical planes in the crust in which stress and deflection have been computed.

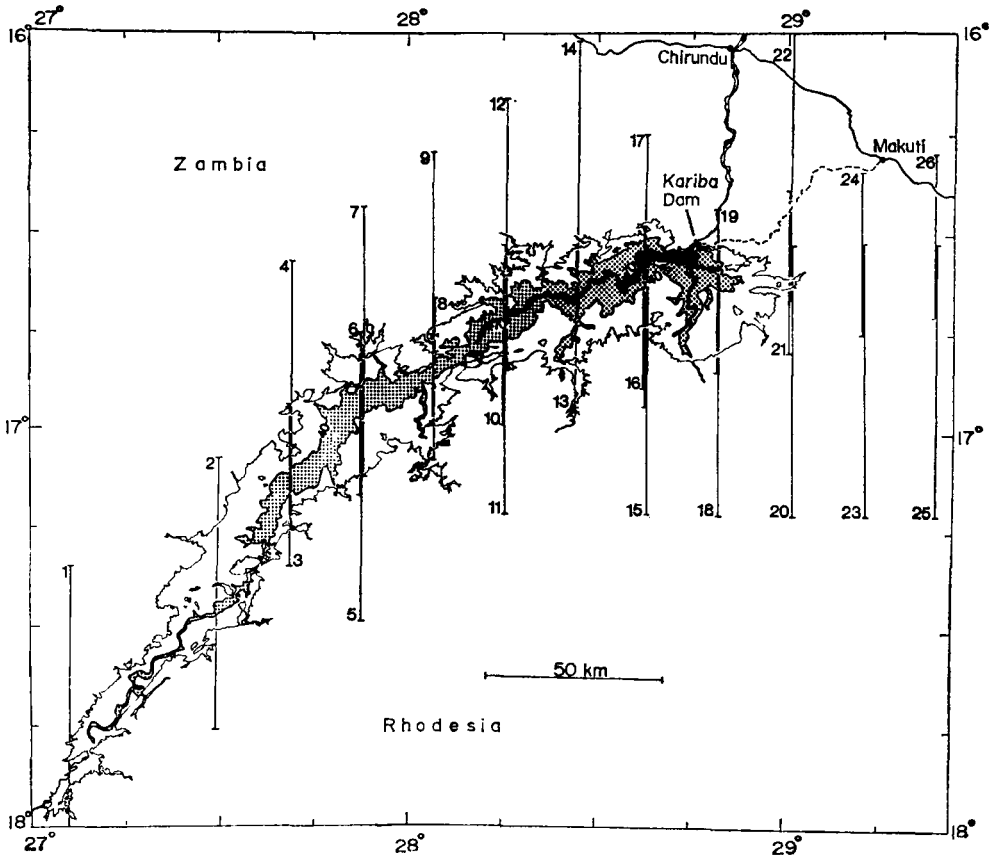

FIG. 1. Simplified bathymetry of Lake Kariba, shown by the shoreline and contours at depths 40 and 70 metres. Numbered lines show sections in which stress and deflection have been computed.

3. Calculation of stress and deflection

The distribution of total stress near an artificial lake cannot be determined because the initial stress is unknown. This paper is concerned with the stress increment caused by the lake. Except when failure is actually occurring, this added stress will be essentially that in an elastic, homogeneous and isotropic medium. Further the sphericity of the Earth has little effect on the stress pattern. Vertical pressures at the ends of the lake converge by only about 2°, and in any case the stress contribution of parts of the lake 200 km from a given point is very small.

In the two-dimensional case most of the integration can be performed analytically and the computation is rapid (Gough 1969). In three dimensions with a lake of irregular shape numerical integration is necessary. The lake is divided into small squares of side a by two sets of orthogonal straight lines, one set conveniently east–west and the other north–south. The mean water depth h in each square is estimated, and the water pressure on the floor of the square is replaced by a vertical force $F = \rho g a^2 h$ acting at the centre of the square. The lake is thus replaced by a two-dimensional array of forces F at spacing a, acting normally to the bounding plane of an elastic half-space.

Clearly the approximation of the lake load by the array of forces will be poor at depths less than the distance a which separates these point forces. In the present work the top row of field points has been taken at depth $4a/3$. This minimum depth may be rather small, but no important errors are introduced because the top row of values is used to continue contours from below in the vertical section, and effects of individual point forces would be obvious. No such effects are seen.

Take axes x eastward, y northward in the plane boundary and z downward. Let F act downward at the origin. The distance from the origin to a point $P(x, y, z)$ is $R = \sqrt{(x^2+y^2+z^2)}$ and $r = \sqrt{(x^2+y^2)}$ is the horizontal projection of R. The stress at P is then given by three normal stresses and one shear stress:

$$\left.\begin{aligned}
\sigma_r &= \frac{F}{2\pi}\left\{\frac{1-2\nu}{r^2}\left(1-\frac{z}{R}\right)-\frac{3r^2 z}{R^5}\right\}\\
\sigma_z &= -\frac{3F}{2\pi}\frac{z^3}{R^5}\\
\sigma_\theta &= \frac{F}{2\pi}(1-2\nu)\left\{-\frac{1}{r^2}+\frac{z}{r^2 R}+\frac{z}{R^3}\right\}\\
\tau_{rz} &= -\frac{3F}{2\pi}\frac{rz^2}{R^5}
\end{aligned}\right\} \qquad (1)$$

where ν is Poisson's ratio and the azimuthal angle $\theta = \arctan(y/x)$ is measured from east through north (Timoshenko & Goodier 1951, p. 364). For convenience in adding the contributions of many forces F, axes are rotated by means of the relations

$$\left.\begin{aligned}
\sigma_x &= \sigma_\theta \sin^2\theta + \sigma_r \cos^2\theta\\
\sigma_y &= \sigma_r \sin^2\theta + \sigma_\theta \cos^2\theta\\
\sigma_z &= \sigma_z\\
\tau_{xy} &= (\sigma_r - \sigma_\theta)\sin\theta\cos\theta\\
\tau_{xz} &= \tau_{rz}\cos\theta\\
\tau_{yz} &= \tau_{rz}\sin\theta.
\end{aligned}\right\} \qquad (2)$$

At a given field point P the stress due to the whole lake is approximated by adding contributions from all the forces F to each of the six stress components σ_x, σ_y, σ_z, τ_{xy}, τ_{xz} and τ_{yz}; the computation proceeds by way of equations (1) and (2) for each force F in turn. Next the principal stresses σ_1, σ_2, σ_3 at P are computed; they are eigenvalues of σ such that

$$\begin{vmatrix} \sigma_x-\sigma & \tau_{yx} & \tau_{zx} \\ \tau_{xy} & \sigma_y-\sigma & \tau_{zy} \\ \tau_{xz} & \tau_{yz} & \sigma_z-\sigma \end{vmatrix} = 0 \tag{3}$$

and the corresponding eigenvectors are the direction cosines l_1, m_1, n_1 of σ_1 and similarly for σ_2 and σ_3 (Jaeger 1956).

Various stress parameters could be chosen for output. We choose the downward normal stress σ_z, the maximum shear stress given by

$$\tau_{\max} = \tfrac{1}{2}(\sigma_1-\sigma_3) \tag{4}$$

and the attitudes of the two orthogonal planes across which $\tau_{\max}$ acts at P. For brevity these will be called the $\tau_{\max}$ planes. The downward normals to them have azimuths

$$\left.\begin{aligned} A_1 &= \arctan\{(l_1+l_3)/(m_1+m_3)\} \\ A_2 &= \arctan\{(l_1-l_3)/(m_1-m_3)\} \end{aligned}\right\} \tag{5}$$

clockwise from north (i.e. from y through x) and the planes are inclined to the horizontal by

$$\left.\begin{aligned} I_1 &= \arctan\left\{\frac{\sqrt{[(l_1+l_3)^2+(m_1+m_3)^2]}}{n_1+n_3}\right\} \\ I_2 &= \arctan\left\{\frac{\sqrt{[(l_1-l_3)^2+(m_1-m_3)^2]}}{n_1-n_3}\right\} \end{aligned}\right\}. \tag{6}$$

The vertical deflection Δd at P due to F is given by

$$\Delta d = \frac{F}{2\pi E}\left\{\frac{(1+\nu)z^2}{R^3}+\frac{2(1-\nu^2)}{R}\right\} \tag{7}$$

where E is Young's modulus (Timoshenko & Goodier 1951). Contributions by all the forces are added to give d at P due to the lake. Finally an estimate of the gravitational potential energy E_g released by the depression is computed. Suppose the field points are arranged in n_x equally spaced north–south vertical planes separated by equal distances Δx, within each plane in n_z rows Δz apart and in each row at n_y points spaced Δy apart. Then E_g for the whole volume of rock

$$n_x n_y n_z\, \Delta x\, \Delta y\, \Delta z$$

represented by the field points can be approximated by

$$E_g = \rho g\, \Delta x\, \Delta y\, \Delta z \sum_n d_n \tag{8}$$

with $n = n_x n_y n_z$. Equation (8) could be generalized for variable spaces between field points but to small advantage. It holds with arbitrary displacements in the y direction of arrays of field points in successive yz planes, because parallelograms on a common base and of equal height have equal areas. Such displacements would be chosen to follow the lake; linear displacements sufficed at Kariba. Deflections

d_1 and d_2 at the two uppermost rows of field points are extrapolated to give an estimate of the contribution E_g' of depression of the top layer of thickness t

$$E_g' = \rho g t \, \Delta x \, \Delta y \sum_m \left[d_1 + \frac{t}{2\Delta z} (d_1 - d_2) \right]_m \tag{9}$$

with $m = n_x n_y$.

Having computed σ_z, τ_{max}, A_1, A_2, I_1, I_2, d and ΔE_g for the first field point, the program stores the first seven parameters in seven arrays, accumulates ΔE_g and proceeds to the next field point. For Lake Kariba, which strikes mainly east–west where it is deep, the field points were chosen in north–south vertical (yz) planes, each of which gives each parameter over a vertical section through the rock roughly transverse to the overlying lake. The lake was divided into 1302 nearly square rectangles $2{\cdot}22 \times 2{\cdot}30$ km. With 1302 point forces and an array $n_y = 51$ by $n_z = 24$ of field points, one north–south section required 14 minutes in an IBM 360–67 system. Twenty-six sections have been used in the study of the full lake. Some of the profiles were also run after reducing the mean water depths in all squares by a decrement Δh; disregarding all squares in which $h - \Delta h < 0$ one very easily secures the stress distribution when the lake stood Δh below its full level. To study the development of stress as the lake filled, runs were made for nine lake levels in all. The results are discussed in Paper II in relation to the seismicity. The time per run was reduced as Δh increased and the number of point forces fell, but in all some 16 hours in the computer were required for the results reported in this paper and in Paper II. A method of calculation of a less brute-force type would be desirable but we have not succeeded in finding one. The Boussinesq method does not appear suited to the initial parameters available.

Each parameter except E_g was printed out in the form of a map of the section given by each yz plane, by means of letters and symbols available in the printer. The method is described by McCracken (1965) and its application has been discussed by Gough (1969).

Parameters assumed in the elastic half-space are 0·27 for Poisson's ratio in all computations, 0·85 megabar for Young's modulus (Birch 1966) in the computation of vertical deflection, and $2{\cdot}7$ g cm^{-3} for the density in computing the gravitational energy released.

4. Incremental stress under the full lake

Stress parameters have been computed in the vertical planes indicated by the lines numbered 1–26 in Fig. 1. Fig. 2 shows the downward normal stress σ_z and maximum shear stress τ_{max} in two north–south planes, P–16 across the Sanyati Basin where the stresses are largest, and P–21 across the eastern extremity of the lake. Fig. 3 shows σ_z and τ_{max} in planes P–3 and P–10, which cross the upper basin and the western part of the lower basin respectively. The frame of each drawing measures 45 km north–south, north on the right, and 37·5 km vertically. The load is at the top of each frame and as explained in Section 3, calculations were not made at depths less than 3 km because they would be inaccurate.

At the planes P–10 (Fig. 3 lower) and P–16 (Fig. 2 upper) the lake approximates a two-dimensional one of triangular section. Comparison of these figures with Fig. 3 of Gough (1969) will show a general resemblance. The two-dimensional case is helpful in extrapolating the present results in the top 3 km layer, left blank in Figs 2 and 3. The σ_z contours clearly continue up to the surface and the τ_{max} contours close beneath the surface, as they must since shear stress vanishes at the lake floor. The largest value of τ_{max} in plane P–16 must approximate the maximum for the lake, at 2·12 bars. This value occurs at about 5 km depth under the Sanyati Basin.

The section P–21 at the eastern extreme of the lake shows that both σ_z and τ_{max} fall rapidly outside the limits of the load; the maximum values noted under the lower parts of Fig. 2 should be compared with those for section P–16. A narrow maximum in σ_z occurs under an arm of the lake. The maximum of τ_{max} goes to mid-crustal depths and broadens as the lake is left. In the upper basin the section P–3 shows very asymmetric distributions of σ_z and τ_{max} (Fig. 3 upper). Local maxima in both parameters occur under the river bed, south of the profile centre. In the northern part of the section, because of the curvature of the lake, the deeper water to the north-east contributes, especially to τ_{max} and, as in plane P–21, mainly at depth; the effect is that the deeper contours swing to the north and produce the asymmetric patterns. The contours are broadened because P–3 is far from normal to the lake strike. Although the maximum values of σ_z (4·15 bars) and τ_{max} (1·80 bars) in plane P–3 are not much lower than those in planes P–10 and P–16 in the lower basin, the large stresses are confined to very small areas in P–3, as the contours show.

In the two-dimensional case the orthogonal planes across which τ_{max} acts (τ_{max} planes) all have strike parallel to the lake axis and can be represented in a single diagram with the magnitude of the shear stress (Gough 1969). In the three-dimensional case this is not convenient, and instead the τ_{max} planes are indicated, in Fig. 4,

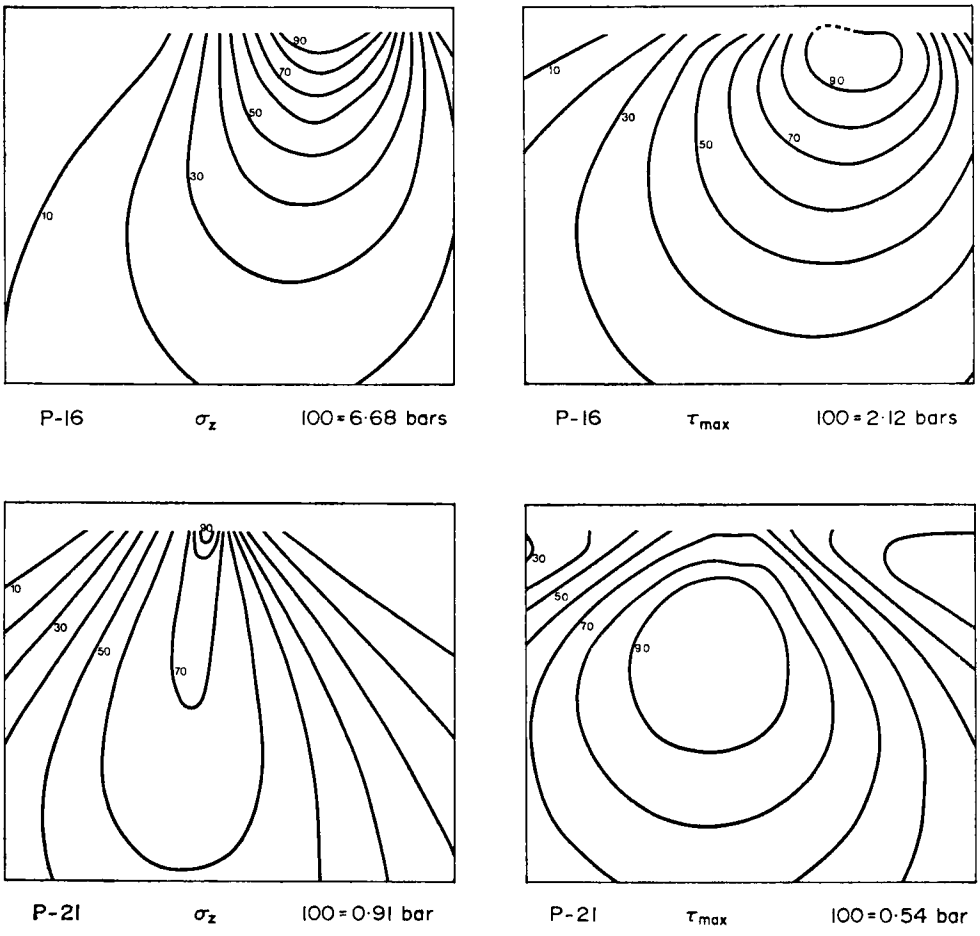

FIG. 2. Downward normal stress (left) and maximum shear stress (right) in two north–south vertical planes. North is at the right. The frames are 45 km N–S by 37·5 deep. Profile numbers refer to Fig. 1.

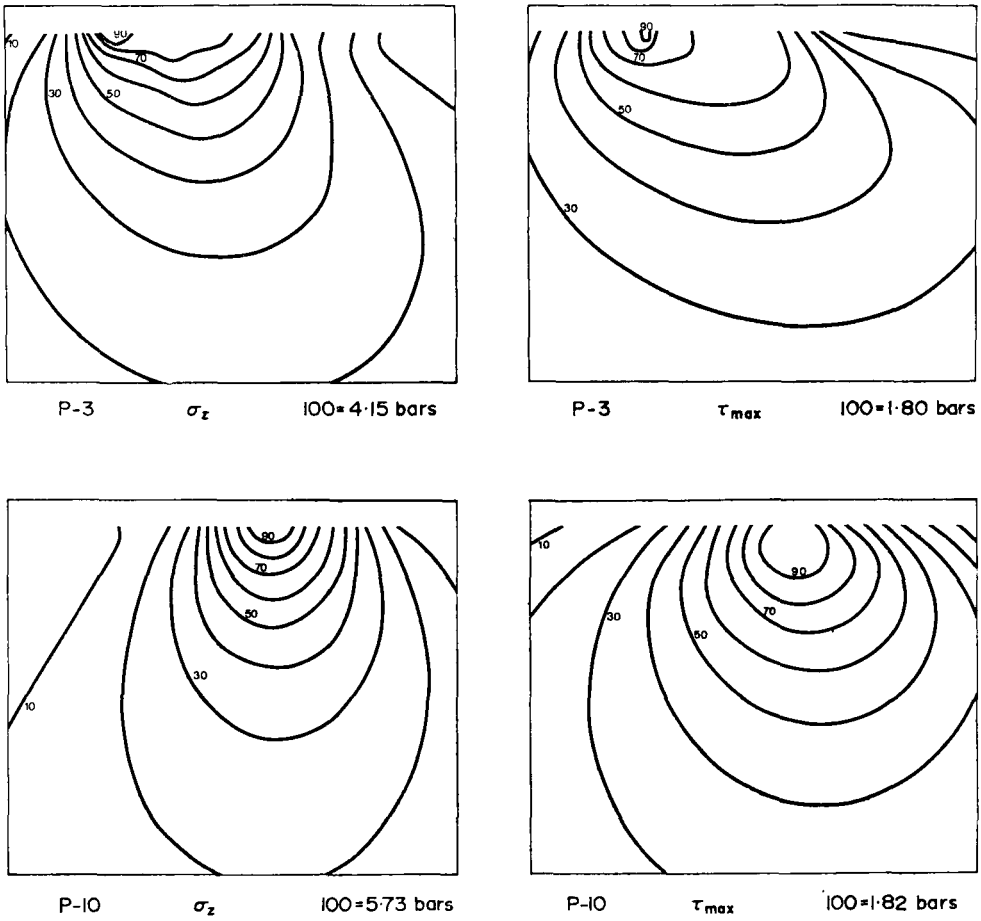

FIG. 3. Downward normal stress (left) and maximum shear stress (right) in two north–south vertical planes. North is at the right. The frames are 45 km N–S by 37·5 km deep. Profile numbers refer to Fig. 1.

at points on six profiles in the horizontal plane at depth 13 km, together with contours of the magnitude of τ_{max} at this depth. The contours are controlled by values in all section planes shown in Fig. 1. The depth 13 km was chosen to avoid local deflections of the τ_{max} planes by small scale irregularities in the lake depth, while still showing over 80 per cent of the maximum value of τ_{max} in the sections through the heavily-loaded basins. It will be seen that there are separate closed 1-bar contours under the upper and lower basins, even at 13 km depth. Where the load approaches a two-dimensional form, in particular along the lines 15–16–17, 11–10–12 and 5–6–7 (Figs 1 and 4), the strikes of the two τ_{max} planes at each point nearly coincide. This shows that the intersection of the two planes is nearly horizontal. The strike closely parallels that of the lake. Along any north–south profile the two planes swing about their nearly horizontal line of intersection. Where τ_{max} has its maximum value the τ_{max} planes dip at $\pm 45°$, and rotate very rapidly as one moves north or south from the centre. The rapid rotation is an effect of the small widths of the deep basins.

The most westerly and easterly profiles show large angles between the strikes of pairs of τ_{max} planes, except near the load. At the end points of these profiles σ_z, which falls rapidly as the lake is left, will no longer be the largest principal stress, and the τ_{max} planes indicate largest and least principal stresses in nearly horizontal planes.

The information given in Fig. 4 on the attitudes of τ_{max} planes forms about one per cent of the total data of this kind in the output from the computer. The paper as a whole gives a similarly small sample of the information yielded by the program.

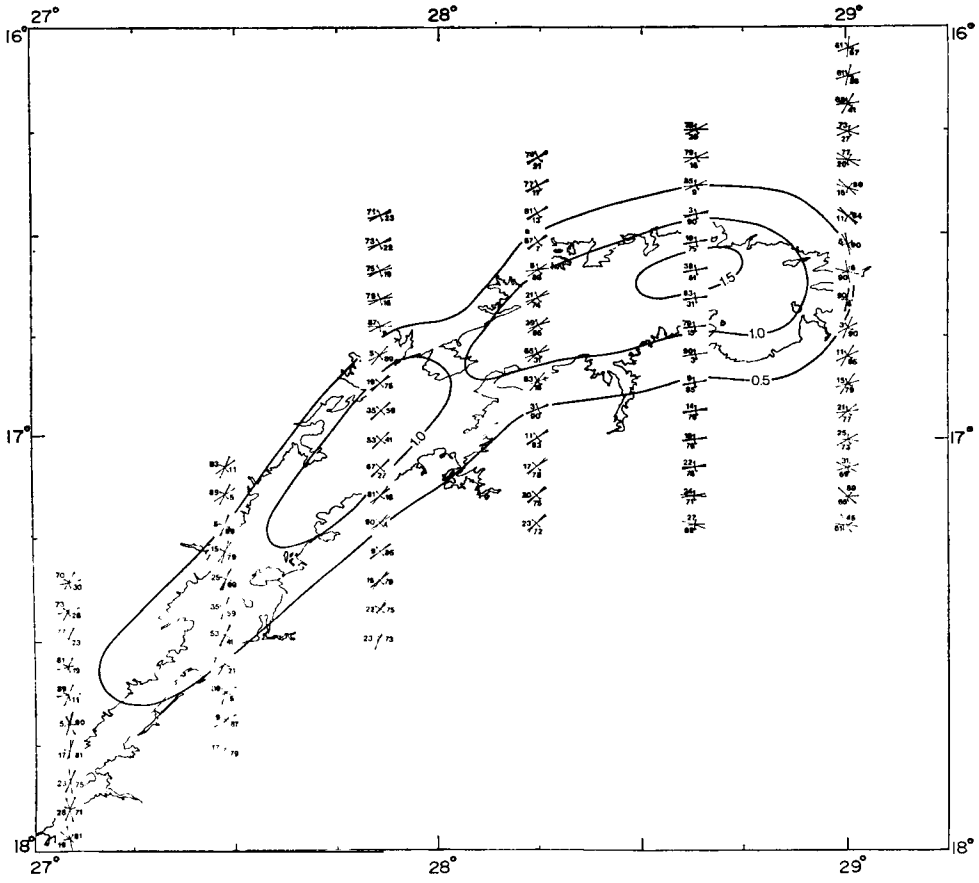

FIG. 4. Maximum shear stress at depth 13 km under Lake Kariba. Contours show magnitude in bars: strike-dip symbols show attitudes of pairs of planes across which τ_{max} acts.

5. Downward elastic deflection of the crust near the full lake

The deflection in four vertical section planes is shown in Fig. 5: the section-plane numbers refer to Fig. 1. Each frame in Fig. 5 measures 75 km south to north (north on the right) by 60·5 km in depth. These figures therefore have greater extent in width and depth than those of Figs 2 and 3 in the ratio 5/3. A striking feature of Fig. 5 is the slow decrease in deflection with distance from the load. Whereas only small stresses penetrate through the crust (Figs 2 and 3) deflections of several cm occur deep in the upper mantle. For a point force equation (7) shows that d is inversely proportional to distance both at the surface and vertically below the point of application of the force, though with different multiplicative constants.

The sections P–5 and P–17 in Fig. 5 show the depression under the upper basin and the Sanyati Basin respectively. Sections P–17 and P–16 (Fig. 2) are coplanar. The maximum deflection in P–17 must approximate that for the lake, at 23·5 cm.

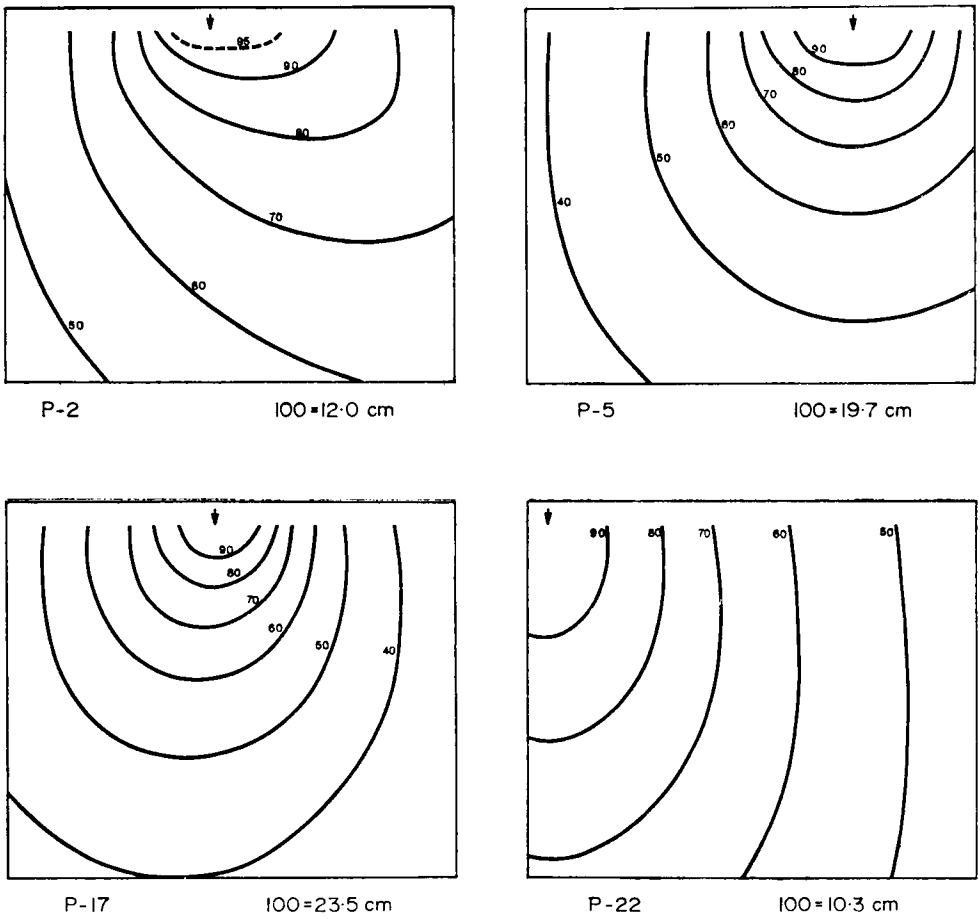

FIG. 5. Downward elastic deflection in four north–south vertical planes under Lake Kariba. Profile numbers refer to Fig. 1. Arrows show location of largest deflection. North is at the right. Frames are 75 km N–S and 60·5 km deep.

The maxima noted in Fig. 5 are at depth 3·0 km; at the surface the value will be slightly greater. Towards the upstream end of the lake deflections are considerable, because of the slow decrease with distance, and at P–2 (Fig. 1) the maximum deflection is half that in the deepest basin (Fig. 5). The same asymmetry appears in the deflection on P–2 as in the shear stress at P–3 (Figs 5 and 3) and is associated with the curvature of the lake. Section P–22 (Fig. 5) has been located to show how the deflection is distributed at distances up to 70 km from the load. In this plane, at the eastern end of the lake, another section-map south of this one (P–20, Fig. 1) showed almost perfect symmetry about the lake axis.

Where the contours in Fig. 5 are nearly straight and vertical, the rock is simply displaced with little or no vertical strain. In these four sections, which are representative of all those studied, it is notable that there is simple displacement without strain above planes dipping outward at 45° from each lake edge. The rock which is strained and contains elastic strain energy is thus virtually all below these 45° planes. A minor point of interest is the small but real increase of the depression with depth in the rock near the surface away from the load. This implies a small tensile vertical stress. While σ_z is always a compression (equation (1)), it increases as z^2 for large r and small z and a small element of rock is extended.

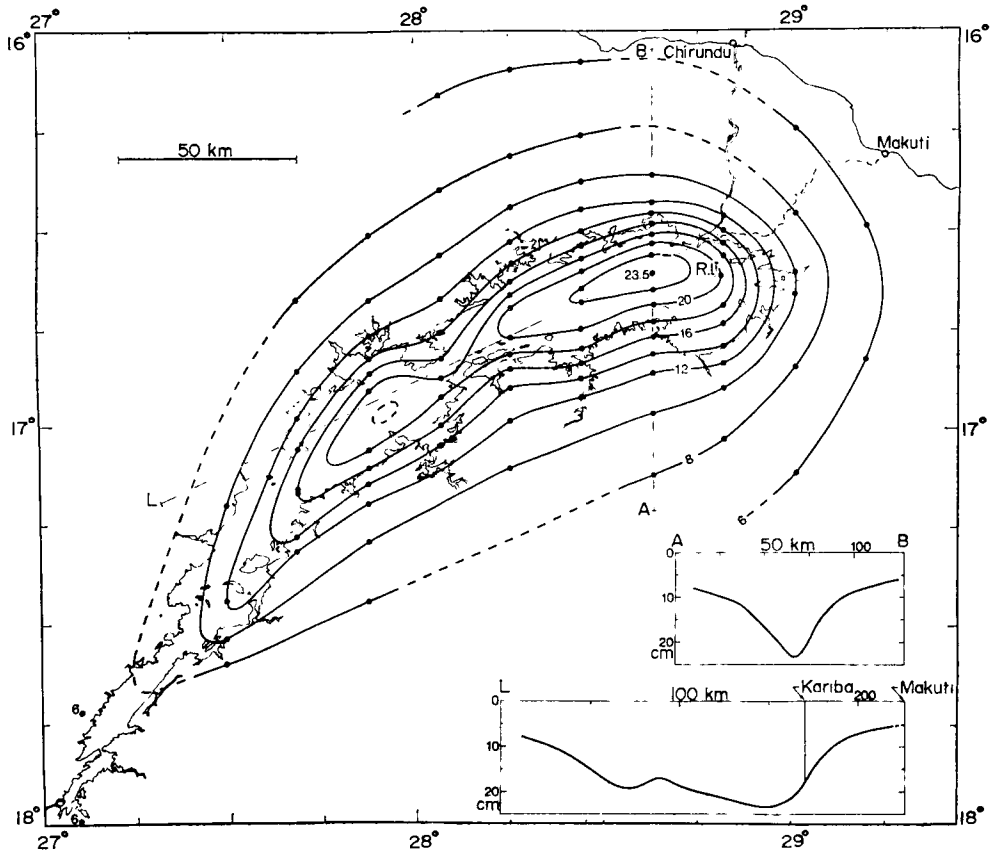

FIG. 6. Calculated downward elastic deflection at depth 3 km under Lake Kariba. Deflections at the surface are slightly larger within the lake. Unit: 1 cm. The dots mark values read from computer output.

Data from all 26 sections have been compiled to yield a contour map of vertical deflection (Fig. 6). It shows the depression at a horizontal plane 3 km deep. That at the surface would be very slightly greater within the lakeshore. The maximum elastic deflection is 23·5 cm in the Sanyati Basin and the 20 cm contour includes the deep water of the lower basin. In the upper basin the maximum appears to be slightly over 20 cm but does not fall in a section plane. The computed depression is shown along transverse (A–B) and longitudinal (L–Makuti) profiles of the lake. The steepest tilts occur close to the north shore near the dam, that is close to the deep Sanyati Basin, and amount to about 6·8 in 10^6 (1·4 seconds).

Before closure of the dam, precise levelling was carried round most of the future shoreline and across the future lake-floor along four lines. This levelling was required for construction of fishing harbours and clearing of bush between the future shoreline and the 30 m depth contour to allow trawl-fishing. The lake levelled routes were linked along four access roads to the primary levelling route along the main road Salisbury–Makuti–Chirundu–Monze–Livingstone–Wankie (Fig. 7). This comprehensive levelling project was carried out by the Department of Trigonometric and Topographic Surveys of the then Federal Government of Rhodesia and Nyasaland, and by subcontractors to that department. Further details have been published by Sleigh, Worrall & Shaw (1969). All routes, except the part of the primary levelling route indicated in Fig. 7, were levelled before the lake began to form.

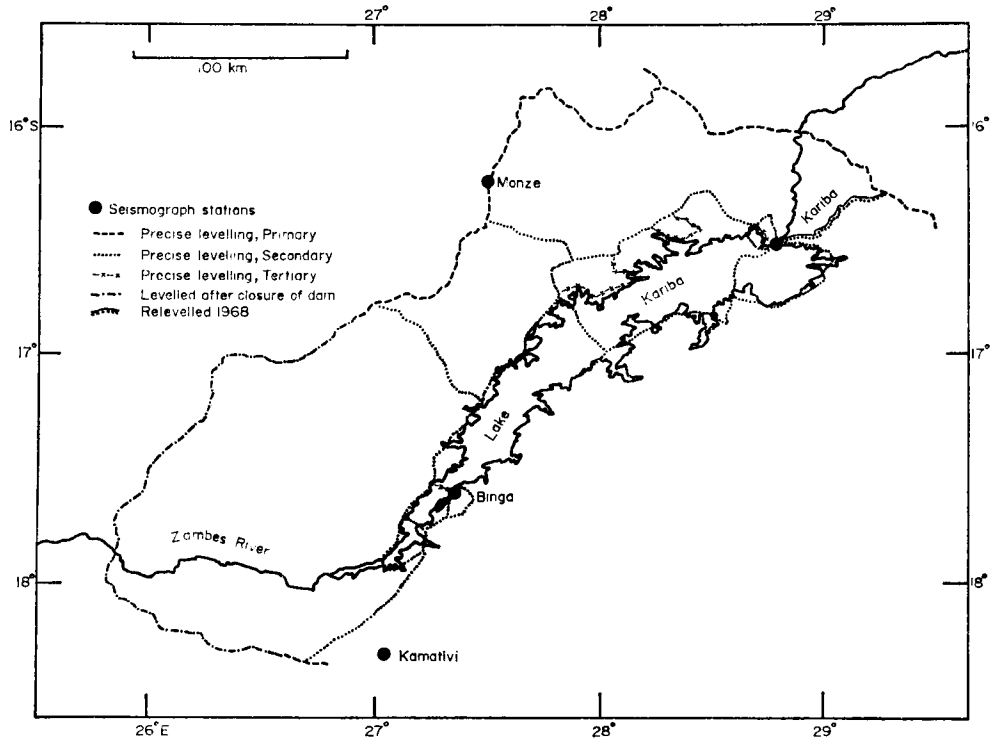

FIG. 7. Precise levelling routes near Lake Kariba. All routes except the indicated part of the primary route were completed before the dam was closed.

The Federal Survey Department started relevelling the road from Kariba to Makuti (Fig. 1) in October 1963, but had not completed the distance when the work was overtaken by the breakup of the Federation on December 31 of that year. This road was relevelled in 1968 by the Department of the Surveyor General of Rhodesia (Sleigh *et al.* 1969). Some of the benchmarks had been destroyed by construction of a new road, but sufficient were re-occupied to give a good picture of the changes. The differences between the 1957 and 1968 levels, relative to Makuti, were plotted by Sleigh *et al.* against the benchmark positions projected on a straight line (their Figs 3 and 5). In Fig. 8 the black dots show the 1957–1968 differences given in Table 2a, Sleigh *et al.* (1969), projected as in their paper on a straight profile.

The 1963 relevelling started at Kariba fundamental benchmark G1F1 on October 10, after the intense seismic disturbance of September 1963. Political events terminated the work at benchmark 35, since destroyed. As Sleigh *et al.* (1969) have shown, the 1963 profile fits very well to that of 1968 if benchmark 39 (Fig. 8) is given the same level in both. There is however one interesting difference. Benchmark G1F1, the fundamental Kariba mark, shows an apparent uplift of 2·9 cm between October 10, 1963 and 1968. This is almost certainly significant in terms of the precision of the work. Smaller uplifts of doubtful significance are shown by benchmarks 74 (1·2 cm) and 75 (1·0 cm) near Kariba. In contrast, five benchmarks out of six between 44 and 71 show subsidence since 1963, three of them by more than 1 cm (marks 44, 66 and 68) (Sleigh *et al.* 1969, Table 2b). While the significance of the changes, other than that at G1F1, cannot be established, the pattern of the differences is suggestive of uplift of a block including Kariba and subsidence of a block further east. While such movements cannot have been associated with the seismic activity of September 1963, which antedated the 1963 relevelling, many tremors occurred

between October 1963 and 1968, including one of magnitude 5·5 (Paper II, Fig. 5(b)) The comparison of the 1963 and 1968 relevellings shows the great value of the 1963 work, which was undertaken under conditions of great discouragement by a Department under sentence of dissolution.

Calculated elastic deflections, estimated by plotting the benchmarks on the large-scale original of Fig. 6, are shown by open circles in Fig. 8. They do not lie on a smooth curve because the road is not straight. In general, the agreement is remarkably good. Between Makuti (21F4) and Kariba (G1F1) both measurement and calculation give 12·7 cm. The precise agreement is of course fortuitous; more significantly, the mean difference for the 27 benchmarks other than Makuti (observed-calculated) is $-0{\cdot}24 \pm 0{\cdot}17$ cm.

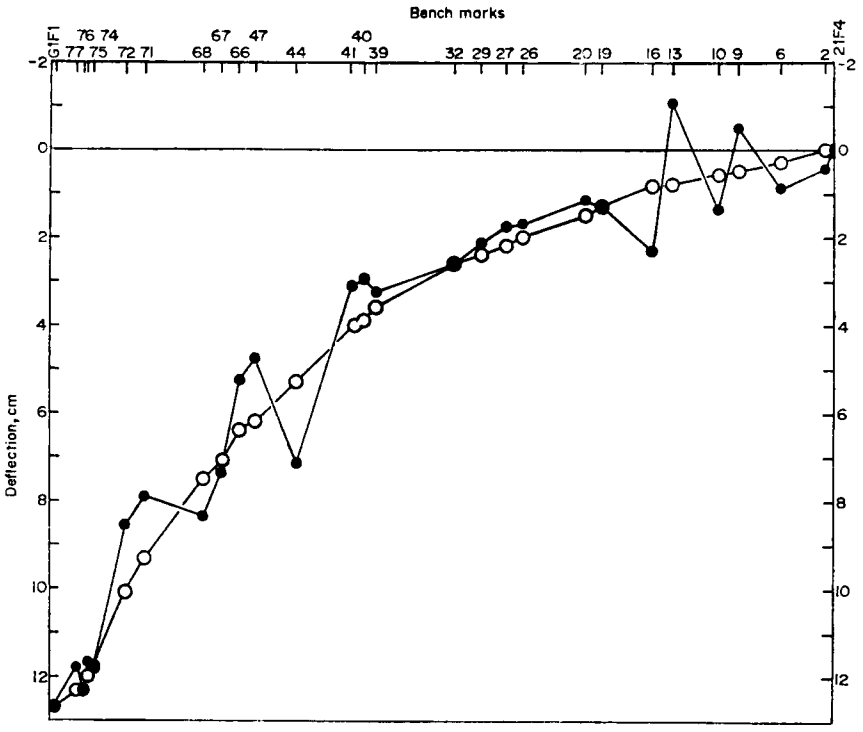

FIG. 8. Measured (dots) and calculated (circles) deflections along route from Kariba (left) to Makuti (right), relative to Makuti.

Several conclusions follow. First, the real deflection is essentially elastic, with superposed disturbance at some benchmarks. Second, the value of Young's modulus (0·85 megabars) assumed in our calculations is representative for the lithosphere in this part of the ancient African shield. This estimate was taken from Birch's Table 7–16 (Birch 1966) which gives values computed from elastic wave velocities at 4 kilobars pressure, by selecting values for acidic crustal rocks. It was not adjusted to fit the data of Sleigh *et al.* Third, Fig. 6 probably gives a valid representation of vertical deflection in the region of Lake Kariba.

The departures from elastic depression are interesting. Those near the lake (benchmarks 44 to 72, Fig. 8) could be related to movements on faults involved in the seismic activity. It is most regrettable that the road-building provides an alternative and leaves the question unanswerable. The inelastic displacements suggested

by Fig. 8, as well as the comparison between the 1963 and 1968 relevellings, suggest that there is a real possibility, by repeating levelling along other routes, of detecting and measuring large strains associated with the earthquakes. In particular a repetition of the levelling network around and across the east end of the lake would have good prospects of detecting motion on faults (Fig. 7 and Paper II, Fig. 3) and should provide extremely interesting results, both as earth science and as highly practical information for dam engineers.

6. Energy conversion

The gravitational energy released as the lake depresses the crust through $d\ (x, y, z)$

$$E_g = g \int\int\int \rho d\, dx\, dy\, dz \tag{10}$$

is stored as elastic energy in the lithosphere. Much of E_g is stored over a vast volume, in rock under very low incremental stress, as can be seen from Figs 5, 2 and 3. If one substitutes for d from (7) in (10) the resulting integral for E_g due to a single point force is non-convergent, so that there is no finite 'total value' of E_g. Physically this implies the unreality of an elastic half-space with uniform gravitational field of semi-infinite extent normal to the bounding plane. The quantity of practical interest is the finite energy E_g which is stored in regions where stress is considerable and where some of E_g may be available for conversion to seismic energy. This part of E_g can be estimated, with a suitable three-dimensional array of field points, by means of equations (8) and (9). Such estimates are considered in Paper II in relation to the induced seismicity. Even if one takes only the top few kilometres of crust immediately under the lake, E_g is much larger than the potential energy $\frac{1}{2}mg\Delta h$ stored because of depression of the lake water itself, and the latter can be neglected.

7. Isostatic adjustment

Lake Kariba is too small a load to depress the crust inelastically so as to restore isostatic compensation. Such adjustment would require flow, and therefore failure, of upper mantle material. Jeffreys (1952) has pointed out that existing mountain ranges could not be supported by a strong crust floating on a fluid mantle, because they would produce stress differences in the crust exceeding its strength. Such major topographic features require strength of order 100 bars in the upper mantle near the M-discontinuity. Stacey (1969) discusses strength in the upper mantle by assuming solid-state creep processes controlled by activation energies. Assuming linear dependences of the creep strength on pressure and on temperature, he uses the best estimates of the radial distributions of p and T to show that the creep strength has a minimum at depth 150–300 km, in agreement with current seismic velocity models. This analysis supports a mantle strength of at least 30 bars at depths less than 50 km. Reference to Fig. 2 (upper right) shows that under the Sanyati Basin at the base of the crust (roughly the bottom of the diagram) τ_{max} reaches 0·75 bars, so the stress difference in the upper mantle will not exceed 1·5 bars. The stress difference probably nowhere exceeds 10 per cent of the strength of the mantle. The lake will therefore produce neither flow in the mantle nor isostatic adjustment.

Acknowledgments

We thank Mr R. W. Sleigh and the Department of the Surveyor-General of Rhodesia for supplying to us a copy of the 1 : 100 000 bathymetric contoured chart of Lake Kariba, and Brigadier M. O. Collins for unpublished data on the 1963 relevelling work. We also wish to thank Mr R. Teshima for writing a subroutine

to determine eigenvalues and eigenvectors in our program, and Mr Fred Schuh of the Computing Centre, University of Alberta for help in the running of the program.

Geophysics Division,
Department of Physics,
University of Alberta,
Edmonton, Canada

References

Birch, F., 1966. *Handbook of Physical Constants*, Table 7–16, p. 169, ed. S. P. Clark, *Geol. Soc. Amer. Memoir* **97.**

Gough, D. I., 1969. Incremental stress under a two-dimensional artificial lake, *Can. J. Earth Sci.*, **6,** 1067–1075.

Gough, D. I. & Gough, W. I., 1970. Load-induced earthquakes at Lake Kariba—II, *Geophys. J. R. astr. Soc.*, **21,** 79–101.

Jaeger, J. C., 1956. *Elasticity, Fracture and Flow*, Methuen and Co. Ltd., London.

Jeffreys, H., 1952. *The Earth*, 3rd edition, Cambridge University Press.

McCracken, D. D., 1965. *A guide to Fortran IV programming*, John Wiley & Sons Inc., New York.

Sleigh, R. W., Worrall, C. C. & Shaw, G. H. L., 1969. Crustal deformation resulting from the imposition of a large mass of water, *Bull. Geodes.*, **93,** 245–254.

Stacey, F. D., 1969. *Physics of the Earth*, John Wiley & Sons, Ltd., Chichester.

Timoshenko, S. & Goodier, J. N., 1951. *Theory of Elasticity*, 2nd edition, McGraw-Hill, London.